ECG-Triggered and Respiratory Gated Image Based B0 Shimming for Single Voxel Spectroscopy of the Myocardium at 3T

Ariane Fillmer[1], Donnie Cameron[2], Thomas W. Redpath[2], Michael P. Frenneaux[2], Dana Dawson[2], and Anke Henning[1,3]

[1]*Institute for Biomedical Engineering, University and ETH Zurich, Zurich, ZH, Switzerland,* [2]*University of Aberdeen, Aberdeen, United Kingdom,* [3]*Max Planck Institut for Biological Cybernetics, Tübingen, Germany*

INTRODUCTION

MR Spectroscopy of the myocardium has strong potential for the investigation and diagnosis of heart disease [1, 2]. As spectral resolution and signal-to-noise ratio in MRS scale linearly with the strength of the static magnetic field, the advantage of higher static magnetic field strength seems obvious; however, with increasing B_0 field strength, challenges such as B_0 field inhomogeneities in the vicinity of the lungs and arteries grow more complex. In order to determine an optimal approach to B_0 shimming of the myocardium for spectroscopy applications, THIS WORK introduces and compares respiratory gated and ECG triggered projection based [3, 4] and image based [5, 6] B_0 shimming as applied to the interventricular septum, along with a rigorous analysis of the acquired proton spectra.

MATERIALS AND METHODS

Measurements were performed in eight healthy volunteers (age 25y – 37y) on a Philips Achieva whole body 3T system (Philips Healthcare, Best, NL) equipped with a full set of 2nd order spherical harmonic shim coils. For signal detection a six channel cardiac SENSE receive coil (Philips Healthcare, Best, NL) was used and an ECG device and a breathing belt were employed to compensate for cardiac and respiratory motion during all calibration phases including B_0 shimming as well as image and spectral acquistions. B_0 shim settings were obtained from a vendor pre-implemented projection based shim algorithm [3], which is closely related to the FASTESTMAP (FM) algorithm, and from an image based shim algorithm, implemented in a modified IDL based Localized Shimming Tool (ST) [5, 6], which has the facility to weight information from a region of interest (ROI) against information from a region of less interest (ROLI) during shim calculation.

In order to position the spectroscopy voxel and estimate the ECG trigger delay, short-axis and 4-chamber cine images of the myocardium were acquired. Additionally, for B_0 shim calculation using the image based algorithm, a B_0 map (10 slices, 3 mm x 3 mm x 3 mm, ΔTE = 1 ms) was acquired without any shim fields applied, using cardiac and respiratory triggering.

Nine non-water-suppressed, PRESS localized spectra (8 averages, TE/TR = 60 ms/2000 ms, no OVS, voxel size [with small variations according to septum size] ≈ 8.5 mm x 57 mm x 44 mm) were then obtained in each volunteer; the first with no shim and the eight others with different 1st and 2nd order B_0 shim settings applied. Two B_0 shim sets were determined by the projection based B_0 shim algorithm and the remaining six were determined by the image based B_0 shim algorithm, which used a number of different shim geometries: only a ROI, where the ROI is the spectroscopy voxel; the ROI along with a rectangular ROLI; and the ROI combined with a ROLI that covered the whole heart (WH ROLI) [6] (see fig. 1). The obtained spectra were then analyzed with regard to line width and line shape. In order to do so, an ideal Voigt line was fitted to the water peak. As in some cases the spectra did show splitting, the FWHM was extracted from the original data as well as from the fit (see table (1)).

Since spectra with heavy line shape distortions require more post processing and are more difficult to reliably quantify, we also considered line shape as a criterion for B_0 shim quality. In order to make a quantitative statement about the line shapes of the spectra, the spectra were normalized to the highest peak value and the Voigt line fit was scaled accordingly. The fit function was then subtracted from the measured data. The area between x axis and the difference curve within a frequency interval of ± 200 Hz around the water peak was then used as a measure for the deviation of the actual line shape from an ideal Voigt line shape.

RESULTS AND DISCUSSION

Figure (2) displays spectra acquired with different linear B_0 shim settings in the septum of a volunteer's heart. The influence of the B_0 shim settings on the line shape and line width is clearly visible. In Figure (3) the FWHM values of spectra obtained with different B_0 shim settings are compared for all volunteers. On average the FWHM is the smallest for the 1st order shim settings obtained by the image based algorithm, when only the ROI is considered, and when the ROI is considered in combination with a WH ROLI. In addition the use of a linear B_0 shim set determined with a WH ROLI, usually results in a line shape that is closest to a theoretical Voigt line, as can be seen in figure (4). This suggests, as has been previously shown [6, 7], that it can be beneficial to take information from the vicinity of the ROI into account for the determination of shim settings, and weight this information if necessary.

However, the consideration of a rectangular ROLI for the B_0 shim determination that intersects both lung and chest wall tissue, compromises the B_0 shim calculation in the ROI significantly and leads to strikingly lower B_0 shim quality compared to other shim sets (fig. (3, 4), tab. (1)).

It can also be seen from the data, that even though a B_0 inhomogeneity correction with 2nd order shim terms should theoretically give better results than a correction limited to linear shim terms only, this is not generally the case for B_0 shimming of the myocardium in reality. In some cases the 2nd order shim set was too poor for proper localization of the spectroscopy voxel and hence, spectral acquisition. The reason for this is most likely respiratory and cardiac motion, which can only be partially compensated for. As linear shim terms are translationally invariant, a little displacement due to motion only adds a small frequency offset, whereas a little displacement with respect to a 2nd order field profile can result in a major B_0 field inhomogeneity [8].

In **CONCLUSION** this work demonstrates the potential for improving the B_0 shim quality for single voxel spectroscopy at 3T in such a challenging region as the myocardium, by employing respiratory gated and ECG triggered image based B_0 shimming including an anatomically conforming ROLI for B_0 shim calculation.

Shim set	FWHM [Hz]	FWHM of fit [Hz]	DEV [a.u.]
no shim	58.0 ± 33.9	60.0 ± 37.2	18.0 ± 10.7
FM shim 1st order	29.9 ± 11.1	29.3 ± 11.0	10.8 ± 10.7
FM shim 2nd order	29.1 ± 11.3	33.5 ± 15.1	12.6 ± 7.1
ST ROI only 1st	25.8 ± 14.4	25.6 ± 13.5	8.5 ± 7.6
ST ROI only 2nd	37.7 ± 41.0	52.9 ± 82.3	8.8 ± 9.3
ST rect. ROLI 1st	48.4 ± 52.0	49.4 ± 47.8	12.1 ± 7.9
ST rect. ROLI 2nd	36.3 ± 14.5	35.5 ± 12.4	20.2 ± 8.8
ST WH ROLI 1st	25.2 ± 13.7	25.1 ± 12.7	6.2 ± 2.8
ST WH ROLI 2nd	24.8 ± 10.6	26.9 ± 11.2	9.7 ± 5.8

Table 1: Mean and standard deviation of the FWHM and the FWHM of the fit of the spectra, as well as the deviation of the actual data from an ideal Voigt line fit in the range of ± 200 Hz around the water peak (DEV) for the different shim sets.

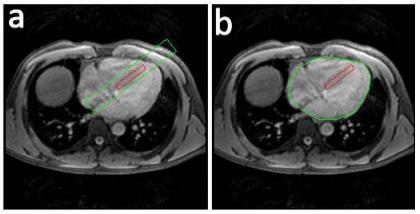

Figure 1: ROI (red) and ROLIs (green) as used by the image based shim algorithm for shim calculation. The ROI is equal to the spectroscopy voxel. (a) rectangular ROLI (b) ROLI that covers the whole heart (WH ROLI)

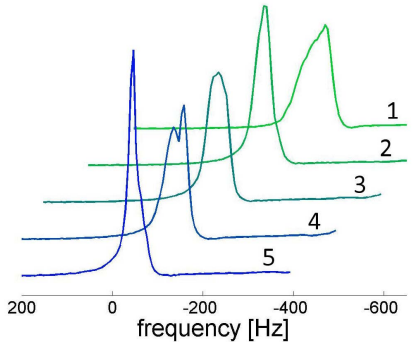

Figure 2: Non suppressed water spectra from the septum of a volunteer's heart acquired with different linear shim but otherwise identical settings. 1: no shim, 2: FM shim, 3: ST shim ROI only, 4: ST shim ROI and rect. ROLI, 5: ST shim ROI and WH ROLI

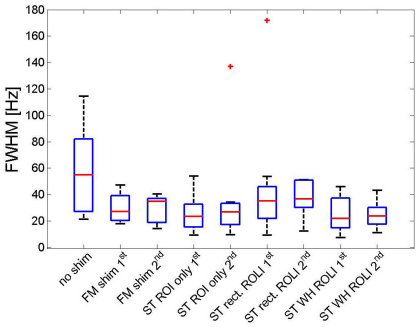

Figure 3: FWHMs from the spectra from all volunteers acquired without any shim, and with 1st and 2nd order FM shim, ST shim ROI only, ST shim ROI and rect. ROLI and ST shim ROI and WH ROLI respectively

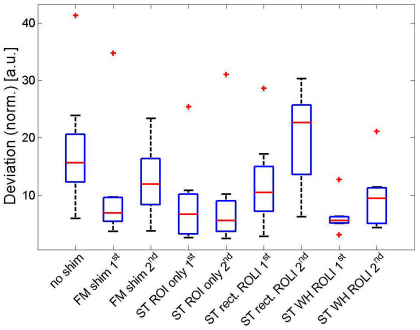

Figure 4: Deviations of the normalized spectra from a fitted Voigt line for different shim settings

[1] J.A. den Hollander et al, MRM 32, 175-180 (1994)
[2] P.A. Bottomley et al, Lancet 351, 714-718 (1998)
[3] A. Hock et al, NMR Biomed, DOI : 10.1002/nbm.2852 (2012)
[4] R. Gruetter, MRM 29, 804-811 (1993)
[5] M. Schär et al, Proc. Intl. Mag. Reson. Med. 10, 1735 (2002)
[6] A. Fillmer et al, Proc. Intl. Mag. Reson. Med. 20, 2065 (2012)
[7] J.C. Siero et al, Proc. Intl. Mag. Reson. Med. 17, 132 (2009)
[8] M.R. Kubach et al, Phys. Med. Biol. 54, N467-N478 (2009)